Food & Function

PAPER

View Article Online
View Journal | View Issue

Cite this: *Food Funct.*, 2019, **10**, 7828

Depolymerized RG-I-enriched pectin from citrus segment membranes modulates gut microbiota, increases SCFA production, and promotes the growth of *Bifidobacterium* spp., *Lactobacillus* spp. and *Faecalibaculum* spp.†

Guizhu Mao,[a] Shan Li,[b] Caroline Orfila,[c] Xuemin Shen,[a] Shengyi Zhou,[a] Robert J. Linhardt,[d] Xingqian Ye[a,e,f] and Shiguo Chen *[a,e,f]

Received 13th July 2019,
Accepted 21st October 2019

DOI: 10.1039/c9fo01534e

rsc.li/food-function

Rhamnogalacturonan-I (RG-I)-enriched pectin (WRP) was recovered from citrus processing water by sequential acid and alkaline treatments in a previous study. RG-I-enriched pectin was proposed as a potential supplement for functional food and pharmaceutical development. However, previous studies illustrated that favorable modulations of gut microbiota by RG-I-enriched pectin were based on *in vitro* changes in the overall microbial structure and the question of whether there is a structure-dependent modulation of gut microbiota remains largely enigmatic. In the present study, modulations of gut microbiota by commercial pectin (CP), WRP and its depolymerized fraction (DWRP) with different RG-I contents and Mw were compared *in vivo*. It was revealed by 16s rRNA high-throughput sequencing that WRP and DWRP mainly composed of RG-I modulated the gut microbiota in a positive way. DWRP significantly increased the abundance of prebiotic such as *Bifidobacterium* spp., *Lactobacillus* spp., while WRP increased SCFAs producers including species in Ruminococcaceae family. By maintaining a more balanced gut microbiota composition and enriching some SCFA producers, dietary WRP and DWRP also elevated the SCFA content in the colon. Collectively, our findings offer new insights into the structure–activity correlation of citrus pectin and provide impetus towards the development of RG-I-enriched pectin with small molecular weight for specific use in health-promoting prebiotic ingredients and therapeutic products.

1. Introduction

Canned citrus segments, instant and delicious fruit products, enjoy a great popularity all over the world, with an annual trade value of almost $900 million (source: UN Comtrade). China accounts for nearly 70% of canned citrus segments on the international market and is the largest citrus planting and harvesting country in the world.[1] However, up to one million pounds of solid waste and effluent water are produced annually in citrus canning processing factories, the latter of which is actually the segment membrane solution that contains a high amount of organic substances (polysaccharides principally), representing both an economic and an environmental challenge.[2] Our previous study recovered pectin with a higher RG-I content from basic water during the segment membrane removal process that occurs in citrus canning factories.[2]

Pectin is mainly composed of structurally distinct regions including homogalacturonan (HG), rhamnogalacturonan-I (RG-I), and rhamnogalacturonan-II (RG-II).[3] HG, whose backbone consists of α-1,4-linked galacturonic acid that is partially methyl-esterified at C-6 and *O*-acetylated in positions 2 and 3, occupies about 65% of commercial pectin. RG-I accounts for 20–35% of commercial pectin and is based on a backbone being formed from a repeating disaccharide of [→2)-α-L-Rha*p*-

[a]*College of Biosystems Engineering and Food Science, National-Local Joint Engineering Laboratory of Intelligent Food Technology and Equipment, Zhejiang Key Laboratory for Agro-Food Processing, Zhejiang Engineering Laboratory of Food Technology and Equipment, Zhejiang University, Hangzhou 310058, China. E-mail: chenshiguo210@163.com; Tel: +86-0571-88982151*
[b]*Institute of Nutrition and Health, Qingdao University, Qingdao 266071, China*
[c]*School of Food Science and Nutrition, University of Leeds, Leeds LS2 9JT, UK*
[d]*Center for Biotechnology and Interdisciplinary Studies, Rensselaer Polytechnic Institute, Troy, New York 12180, USA*
[e]*Fuli Institute of Food Science, Zhejiang University, Hangzhou 310058, China*
[f]*Ningbo Research Institute, Zhejiang University, Hangzhou 315100, China*
†Electronic supplementary information (ESI) available. See DOI: 10.1039/c9fo01534e

(1 → 4)-α-D-GalA*p*-(1→] residues with neutral side chains attached to the O-4 position and sometimes the O-3 position of the α-L-Rha*p* backbone units.[4] The uniform extraction of commercial pectin uniformly aims at maintaining more HG content for best quality control and better application in the food industry as a gelling agent, thickening agent, stabilizer, emulsifier, and color-protecting agent.[5–7] However, during the harsh extraction conditions, the RG-I region is mostly destroyed,[8] which is increasingly gaining attention because of its bioactivity including anti-galectin-3 activity (a lectin associated with cancer progression and metastasis),[7] antitumor activity,[9] immunomodulation ability,[10] and prebiotic activity.[11,12] Structural features, including RG-I content, neutral sugar content, neutral side chain length and variable linking types, and molecular weight (M_w), to some extent, determine the suitability of pectin for specific applications.[5,13]

The structural diversity of pectin and the increasing concern regarding RG-I have recently aroused more interest in rethinking the relationship between pectin's structure and function. Gut microbiota play fundamental roles in the modulation of the host's metabolism, nutrition and immunity.[14,15] Gut microbiota impairment is tightly linked to various diseases and metabolic disorders including inflammatory bowel disease,[16,17] diabetes,[18,19] non-alcoholic fatty liver disease (NAFLD),[20] hypertension,[21] obesity,[22,23] and cardiovascular disease.[23,24] Restoring the disrupted gut microbiota through personalized colonization with prebiotics represents an effective strategy for the management of gut microbiota-related diseases.[25,26] Accumulating evidence illustrates that non-digestible carbohydrates in the daily diet can alleviate and treat disease through modulating the gut microbiota composition.[27] Therefore, elucidating the effect of pectin as a dietary supplement on gut microbiota would be significantly beneficial for clarifying its functional mechanisms. The RG-I region is a highly complex part of pectin and is reported to be potentially used as prebiotics and gastrointestinal drug delivery microcapsules.[28,29] Previous studies reported that citrus pectin has *in vitro* prebiotic activity by stimulating the growth of *Bifidobacterium bifidum*, *Lactobacillus paracasei*, *Bacteroides plebeius*, and *Ruminococcus gnavus* during *in vitro* fermentation.[12,13,30] Besides, the favourable changes in the microbiota composition after pectin supplementation depend greatly on the RG-I content, neutral sugar composition, the degree of esterification and branching.[13] However, the structure–function relationship of pectin has rarely been evaluated *in vivo*.

Considering the remarkable non-digestibility of citrus pectin in the upper gastrointestinal tract,[12,31,32] we have investigated the relationship between the structure of pectin and the modulation of gut microbiota *in vivo*. In our study, the basic structure and chain conformation of CP, WRP, and DWRP were investigated by NMR, SEC-MALLS and AFM. C57BL/6J mice were administered with CP, WRP and DWRP at a dosage of 100 mg kg^{-1} day^{-1}, and the effects on the gut microbiota composition and SCFAs were studied using 16S rRNA and gas chromatography (GC). The diversity and composition of gut microbiota were compared at the phylum, class, family and genus levels and the spatial structural differences in gut microbiota were also investigated. Our study indicates distinct modulations of gut microbiota by different types of pectin and provides theoretical foundations for developing RG-I-enriched pectin as a health-promoting and therapeutic ingredient in prebiotics.

2 Materials and methods

2.1 Materials and preparation of pectin

Citrus segment materials (*Citrus unshiu Marc.*), recovered from basic water from the canning process, were provided by a citrus fruit canning factory in China. The material was washed 2–3 times with 95% (v/v) food-grade ethanol for desalting, the pectin was precipitated and oven-dried at 55 °C for 24–36 h and was abbreviated as WRP. DWRP was degraded from WRP based on the metal-free Fenton reaction, relying on H_2O_2/ascorbic acid, adapted from a previous study.[33] Briefly, the reaction conditions were 200 mM H_2O_2, 20 mM ascorbic acid and temperature at 45 °C. The WRP (5000 mg) starting material was dissolved in 1000 mL ultrapure water, H_2O_2 and ascorbic acid were then added with mixing and the reaction was maintained at 45 °C for 30 min. The depolymerized products were desalted by dialysis using a 500 Da cut-off membrane for 72 h under flowing water, concentrated and subsequently lyophilized to obtain refined samples for further study.

2.2 Structural analysis of pectin

2.2.1 Primary structure of CP, WRP, and DWRP. The primary structures of the three pectin types were studied by HPLC, FTIR, and NMR. Monosaccharide standards, 1-phenyl-3-methyl-5-pyrazolone (PMP), D_2O and commercial pectin from citrus peel (abbreviated as CP) were all purchased from Sigma-Aldrich (Shanghai, China). All other used chemicals were of analytical grade. Chemical compositions of CP, WRP and DWRP (Table 1) were determined according to previously described methods with modifications.[34] FTIR and NMR analysis were conducted based on the method of a previous report.[8]

2.2.2 Chain conformation of CP, WRP, and DWRP. Chain conformations of the three pectin types were studied by SEC-MALLS and AFM. For size exclusion chromatography with multi-angle laser light scattering (SEC-MALLS) analysis, pectin was dissolved in 0.2 M NaCl solution at a concentration of 5 mg mL^{-1}, then 50 μL of the solution was injected through a sample loop after filtering through a syringe-filter (pore size was 0.22 μm). The molar mass and root mean square (RMS) radius of gyration was determined through high-performance (HP) size exclusion chromatography (SEC), with multi-angle laser light scattering (MALLS) (Wyatt Dawn Heleos-II, USA) and an RI detector at 25 °C. Isocratic elution with 0.2 M NaCl solution at a flow rate of 0.5 mL min^{-1} was performed on combined columns including Shodex OH SB-G (pre-column), Shodex SB-806 HQ and Shodex SB-804 HQ (Showa Denko KK,

Table 1 Monosaccharide compositions of CP, WRP and DWRP

Pectin	Molar ratio of monosaccharide								HG (%)	RG-I (%)	HG/RG-I	Rha : (Gal + Ara)
	Man	Rha	GluA	GalA	Glu	Gal	Ara	Fuc				
CP	0	4.45 ± 0.38	0.37 ± 0.02	56.99 ± 0.69	10.15 ± 0.03	13.03 ± 0.12	13.84 ± 0.14	0.20 ± 0.02	52.55 ± 1.07	35.77 ± 1.02	1.47 ± 0.07	1 : 6
WRP	2.16 ± 0.17	3.61 ± 0.16	0.25 ± 0.01	28.64 ± 0.85	0.75 ± 0.06	14.27 ± 0.16	48.94 ± 0.81	1.37 ± 0.16	25.03 ± 0.98	70.44 ± 1.22	0.36 ± 0.02	1 : 20
DWRP	0	6.64 ± 0.08	0.18 ± 0.02	48.93 ± 1.01	0.46 ± 0.05	9.43 ± 0.52	33.58 ± 0.83	0.07 ± 0.02	42.29 ± 1.08	56.29 ± 1.50	0.75 ± 0.04	1 : 6

The molar percentage of homogalacturonan(HG) and rhamnogalacturonan of type I (RG-I) were calculated as the following formula: HG (%) = GalA(mol%) − Rha (mol%). RG-I (%) ≈ 2Rha (mol%) + Ara(mol%) + Gal(mol%). The Rha : (Gal + Ara) ratio stands for the degree of the side chain branching.

Japan). The molar mass was calculated based on the d*n*/d*c* value of 0.0880 mL g^{-1}.

For atomic force microscope (AFM) analysis, pectin was dissolved in ultrapure water at a concentration of 1 mg mL^{-1} with continuous stirring for 2 h and incubation at 60 °C. The stock solutions were then diluted with sodium dodecyl sulphate (SDS) solution to obtain a mixed solution containing pectin and SDS, both at a concentration of 10 μg mL^{-1}. The diluted solutions were then stirred for 24 h and filtered through a syringe-filter (pore size of 0.22 μm). After the samples were ready, 10 μL of pectin solution was moved to three freshly cleaved mica substrates using a micropipette. The three mica substrates were air-dried and observed by AFM (XE-70, Park Scientific Instruments, Suwon, Korea), using the taping mode, in air at room temperature (humidity: 50%–60%). The probe is a classical silicon cantilever (Appnano AN-NSC10) with a spring constant of 37 N M^{-1} and a resonance frequency of approximately 300 kHz. Nanoscope Analysis software was used for image manipulation.

2.3 Animals and experimental design

All procedures were approved by the Institutional Animal Care and Use Committee of Zhejiang University School of Medicine. Forty C57BL/6J male mice (SPF, 6–8 weeks old, IACUC-20180917-02) were purchased from Zhejiang Chinese Medical University Laboratory Animal Research Center. The mice were kept under specific-pathogen-free conditions in a 12-hour light/dark cycle with free access to food and sterile drinking water (DW) in a temperature-controlled room (21 °C ± 2 °C).

Before starting the experiments, the mice were housed 25 per cage and were exchanged multiple times in order to make the fecal microbiome homogeneous. After one week of acclimatization, the mice were randomly divided into four groups: CD group, CD-CP group, CD-WRP group and CD-DWRP group (10 mice per group, 5 mice per cage) and fed for 9 weeks with the standard chow diet (Rodent diet, SHOBREE, Jiangsu Synergy Pharmaceutical Biological Engineering Co, Ltd, Nanjing China). Mice were supplemented daily with 200 μL of sterile water (vehicle), CP (100 mg kg^{-1} d^{-1}), WRP (100 mg kg^{-1} d^{-1}) or DWRP (100 mg kg^{-1} d^{-1}) *via* intragastric gavage. The compositions and energy densities of the diets are listed in Table S2.† The body weight was measured weekly, food intake was recorded daily. At the time indicated, the mice were fasted for 12 hours and anaesthetized, and whole blood was collected from the orbital plexus, then, the mice were sacrificed. Epididymal white adipose tissues, liver, small intestine, caecum and colon samples were removed and weighed. Caecal contents were collected in Eppendorf tubes and immediately stored at −80 °C for subsequent analysis. The intestinal tissue index was calculated using the following formula: intestinal tissue index = intestinal tissue weight/body weight.

2.4 Biochemical analysis and cytokine measurements of serum

Serum was isolated by centrifugation (4 °C, 12 000*g*, 10 min). Total serum cholesterol and triacylglycerol concentrations were

determined using commercial kits (Nanjing Jiancheng Bioengineering Institute, Nanjing, China) according to the manufacturer's instructions. TNF-α, LPS and insulin levels were then quantified using commercial ELISA kits (Cloud-clone Crop, USA).

2.5 16S rDNA analysis

Five samples of each group were randomly selected for 16S rRNA analysis. DNA was extracted from the caecal solid contents of mice by using the E.Z.N.A. ®Stool DNA Kit (D4015, Omega, Inc., USA) according to the manufacturer's instructions. The total DNA was eluted in 50 μL of elution buffer and stored at −80 °C until measurement in the PCR by LC-Bio Technology Co. Ltd. The V3–V4 region of the prokaryotic (bacterial and archaeal) small-subunit (16S) rRNA gene was amplified with slightly modified versions of primers 338F (5′-ACTCCTACGGGAGCAGCAG-3′) and 806R (5′-GGACTACHVGGGTWTCTAAT-3′).[35] The 5′ ends of the primers were tagged with specific barcodes per sample and sequencing universal primers.

The PCR products were purified by AMPure XT beads (Beckman Coulter Genomics, Danvers, MA, USA) and quantified by Qubit (Invitrogen, USA). The amplicon pools were prepared for sequencing and the size and quantity of the amplicon library were assessed on Agilent 2100 Bioanalyzer (Agilent, USA) and with the Library Quantification Kit for Illumina (Kapa Biosciences, Woburn, MA, USA), respectively. The PhiX Control library (v3) (Illumina) was combined with the amplicon library (expected at 30%). The libraries were sequenced on 300PE MiSeq runs and one library was sequenced with both protocols using the standard Illumina sequencing primers, eliminating the need for a third (or fourth) index read.

Samples were sequenced on an Illumina MiSeq platform according to the manufacturer's recommendations, provided by LC-Bio. Paired-end reads were assigned to samples based on their unique barcode and were truncated by cutting off the barcode and primer sequence. Paired-end reads were merged using FLASH. Quality filtering on the raw tags was performed under specific filtering conditions to obtain clean high-quality tags according to the FastQC (V 0.10.1). Chimeric sequences were filtered using Verseach software (v2.3.4). Sequences with ≥27% similarity were assigned to the same operational taxonomic units (OTUs) by Verseach (v2.3.4). Representative sequences were chosen for each OTU, and taxonomic data were then assigned to each representative sequence using the RDP (Ribosomal Database Project) classifier. The differences in the dominant species in different groups were determined and multiple sequence alignment was conducted using the PyNAST software to study the phylogenetic relationship of different OTUs. Information on the OTU abundance was normalized using a standard of sequence number corresponding to the sample with the least sequences. Alpha diversity was applied to analyze the complexity of the species diversity for a sample through 4 indices, including Chao1, Shannon, Simpson and observed species. All these indices in our samples were calculated with QIIME (Version 1.8.0). Beta diversity analysis was used to evaluate the differences in samples in species complexity. Beta diversity was calculated by principal coordinates analysis (PCoA) and cluster analysis using QIIME software (Version 1.8.0). Spearman's rho non-parametric correlations between the gut microbiota and heal-related indexes were determined using R packages (V2.15.3).

2.6 Caecal and colonic short-chain fatty acids

Short-chain fatty acids (SCFAs), including acetate, propionate and butyrate, were measured in caecal and colonic samples using an external standard method described by Wu T. R. *et al.*[36] with minor modifications. Briefly, the caecal contents (70 mg) of each animal were suspended in 700 μL of 0.01 M PBS, and mixed intermittently on a vortex mixer for 10 min and then centrifuged at 12 000*g* for 5 min at 4 °C. The supernatants were acidified with an equal volume of 0.1 M H_2SO_4 and extracted with 800 μL of ethyl ether. The contents of SCFAs were measured in the organic phase using a gas chromatograph (Agilent Technologies, Stockport, UK) equipped with a 30 m × 0.25 mm × 0.25 μm HP-INNOWax column (no. 19091N-133; Agilent Technologies, USA) and flame ionization detector (Agilent Technologies). The determination program for SCFAs was as follows: the temperatures of the injector and detector were 240 °C and the column temperature was 200 °C; split injection (20 : 1). The initial column temperature was 110 °C and was maintained for 5 min, thereafter increasing at a rate of 20 °C min^{-1} until reaching 240 °C, and was held there for 5 min. The flow rates of N_2 (carrier gas), H_2 (make-up gas), and air were 20, 15 and 150 mL min^{-1}, respectively. SCFAs of all samples were quantified by comparing the peak areas with those of chemical standards.

2.7 Statistical analysis

Data were expressed as means ± SD. Statistical analysis was performed using GraphPad Prism V.7.04 (GraphPad Software, USA). One-way analysis of variance (ANOVA) for multiple comparisons was conducted, followed by the non-parametric Kruskal–Wallis test with Dunnett's multiple comparisons test. Significance was set at $p < 0.05$.

3 Results and discussion

3.1 Pectin structure analysis

CP, WRP and DWRP are mainly composed of galacturonic acid, rhamnose, galactan, arabinan, glucuronic acid, fucose, glucose (Table 1), in different proportions. CP had the highest HG content (52.55%), followed by DWRP (42.29%) and WRP (25.03%). Conversely, WRP had the highest RG-I content (70.44%), followed by DWRP (56.29%) and CP (35.77%). WRP had the highest degree of branching with a Rha : [Gal + Ara] ratio of around 1 : 20, the branches were dominated by arabinan, while CP and DWRP had lower arabinan. Despite the differences in the HG/RG-I content, CP and WRP both have similarly large M_w of around 500 kDa (Table S1†), while DWRP has a low M_w of 12.1 kDa (Fig. S1†). According to FTIR

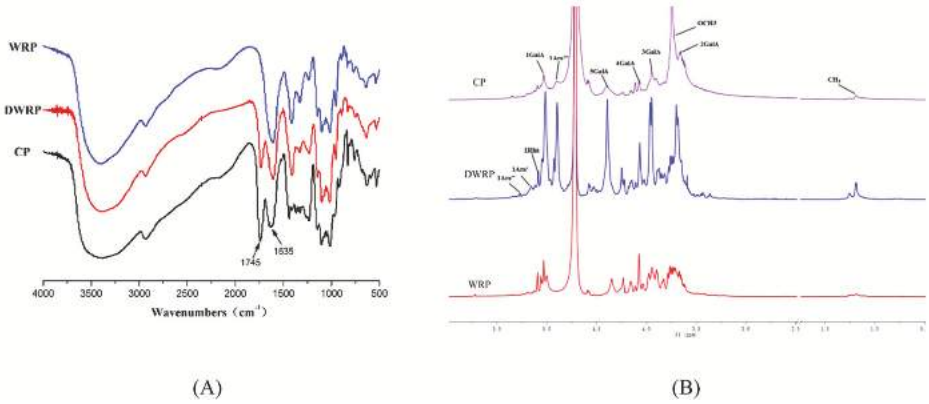

Fig. 1 The primary structure of CP, WRP and DWRP; (A) FTIR spectra of the three pectin types; (B) the ^{1}H NMR spectrum of the three pectin types.

(Fig. 1A), both CP and DWRP gave an obvious absorbance at 1745 cm^{-1} (COO-R) and 1635 cm^{-1} (COO–), only the WRP showed a sole absorption peak at 1635 cm^{-1}, confirming that WRP had the highest RG-I content. Detailed structural information about the proton environment of CP, WRP and DWRP was obtained by ^{1}H NMR (Fig. 1B). Five major signals were assigned to the proton in the D-galacturonic acid: H-1, 5.03 ppm; H-2, 3.66 ppm; H-3, 3.93 ppm; H-4, 4.07 ppm and H-5, 4.35 ppm, respectively.[37] In the anomeric region, the signal at 5.03 ppm was attributed to the H-1 of rhamnose,[9] which was obvious in the spectra of both WRP and DWRP. The signals between 5.07 and 5.20 ppm were attributed to the H-1 of different types of arabinan.[8] Therefore, CP, DWRP and WRP were shown to have successively larger signals for arabinan, consistent with the monosaccharide composition. Besides, the spectra from WRP and DWRP showed additional peaks that were hard to assign, probably due to the presence of larger amounts of Ara, Gal, and Rha, almost equal to that of GalA.

SEC is most appropriate for macromolecules with large M_w. Conformation plots of CP and WRP in 0.2 M aqueous NaCl solution were calculated from the slope between the RMS radius and the molar mass (Fig. 2A). The slope value of the linear fitting for CP and WRP was 0.12 and 0.05, respectively, predicting the branched conformation consistent with the anomalous SEC phenomenon of plots bending upward at the low molar mass region.[38,39] The Mark–Houwink–Sakurada equation (MHS, $[\eta] = KM_w^{\alpha}$) was used to determine the chain conformation of macromolecules.[40] The values for CP and WRP were $[\eta] = 0.22M_w^{0.61}$ (mL g^{-1}), $[\eta] = 0.58M_w^{0.45}$ (mL g^{-1}), respectively (Fig. 2B). According to the literature, values of α ranging from 0–0.3, 0.5–0.8, 1 and 1.8–2 correspond to chain conformations that are spherical, random coiled, semi-rigid and rods, respectively.[38,41] CP and WRP had α values of 0.61 and 0.45, respectively, indicating a higher branched-chain structure of WRP.

AFM was used to determine the molecular shapes of CP, WRP and DWRP (Fig. 2). The micrographs show that the chain-like structure is characteristic of all the pectins. WRP appeared significantly more branched than CP and DWRP, with the interlaced structure of a network. CP and DWRP were shown to have successively higher linear and sparse branches as compared to WRP, consistent with the chromatograms of the chain conformation. The expected diameters of single polysaccharide strands, imaged by AFM and adopting helical conformations, ranged from 0.5 to 0.8 nm.[42] The diameters of CP, WRP and DWRP were calculated as 0.58 nm, 0.75 nm and 1 nm, respectively, suggesting that DWRP is probably slightly aggregated.

3.2 Effects of pectin with different RG-I content on the structure of the gut microbiota community

The RG-I region can be partially degraded by specific gut microbes including *Bacteroide thetaiotaomicron*, *Bifidobacterium Longum.*[43] Nevertheless, the effect of RG-I on the composition and diversity of the gut microbiota *in vivo* is unknown. We investigated and compared the effects of pectin, differing in RG-I content, M_w and conformation, on the gut microbiota profile in mice.

C57BL/6J mice underwent a nine-week dietary treatment consisting of conventional chow supplemented with the three pectin preparations. High-throughput sequencing was adopted to characterize the diversity of the caecal microbiota at the end of the nine-week intervention. Surprisingly, the caecal gut community richness and diversity after the interventions with large M_w pectins (CD-CP and CD-WRP) were not significantly different from the standard chow (CD), as demonstrated by Chao1, Shannon and Simpson (Table S3†). The CD-DWRP significantly decreased the richness and diversity of the caecal microbiota. In accordance with our observation, the oral administration of Lentinula edodes-derived polysaccharides also significantly decreased the diversity and the amount of OTUs (Operation Taxonomic Units) in caecal microbiota.[44] As for RG-I-enriched pectin (Fig. S3†), we tentatively put forward that this was probably due to the relative enrichment effects of some beneficial bacteria, while the destructive bacterial were reduced because of the antibacterial effects, which was proposed by the previous studies.[30,45–47] Nevertheless, the exact

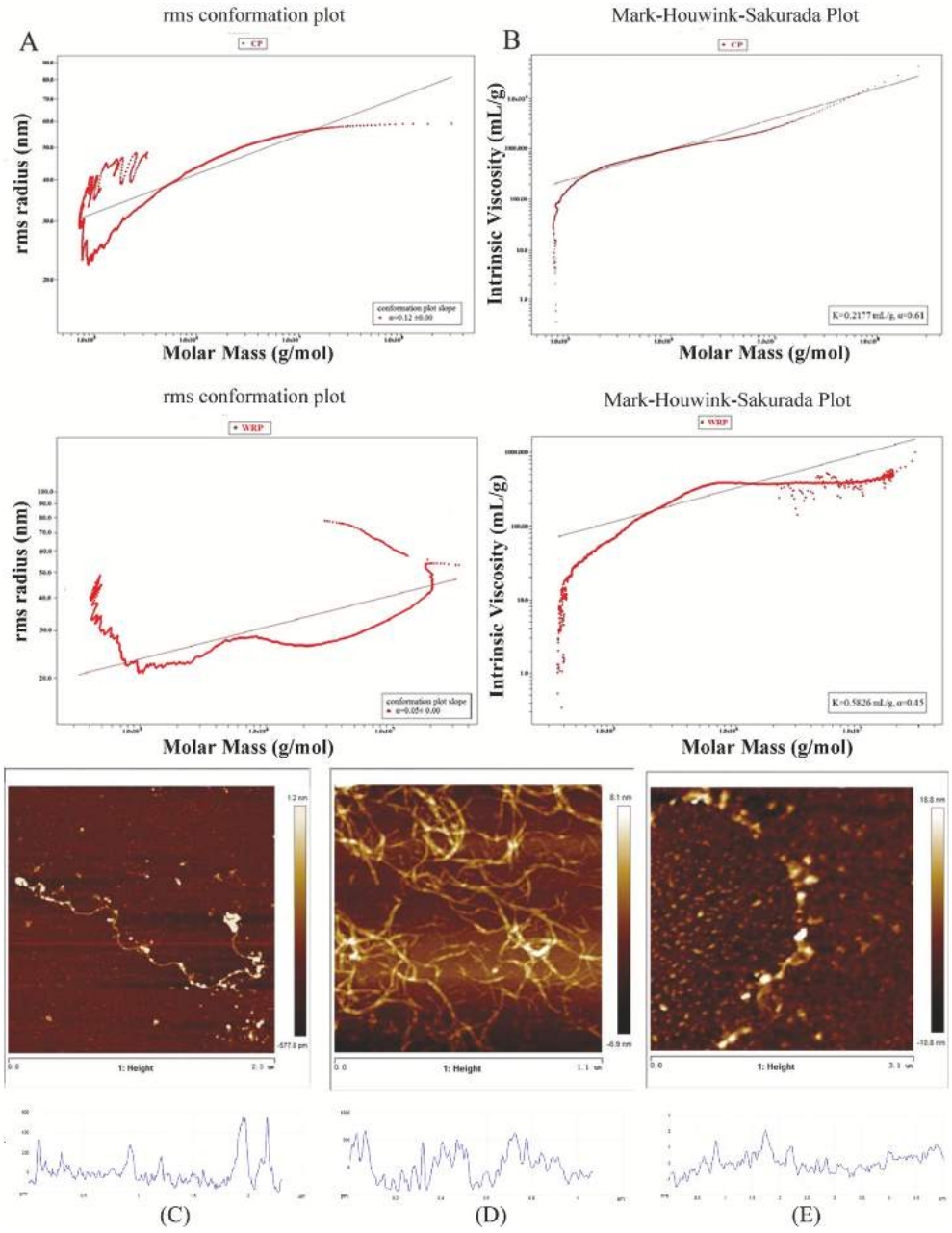

Fig. 2 The chain conformation of CP, WRP, and DWRP. (A) Conformation plots of CP and WRP in 0.2 M aqueous NaCl solution at 25 °C. (B) The relationship between R_g and M_w, the Mark–Houwink–Sakurada equation. Representative topographical AFM images of (C) CP, (D) WRP and (E) DWRP.

explanation needs further detailed analysis of specific microbial species.

Based on clustering analysis (Fig. S2†), supplementation with pectins led to changes in the clusters of microbial groups, as compared to standard chow. The groups were further analyzed and compared using principal component analysis (PCA) and 3D-principal coordinate analysis (3D-PCoA). As shown by PCA, the three pectin types changed the structure of the gut microbiota in different ways (Fig. 3). With a greater distinction in segregation, 3D-PCoA depicted that the CD-WRP group showed a more pronounced microbiota structural shift than that of CD-CP and CD-DWRP groups all along the first, second, and third principal coordinates (Fig. 3b), as compared to CD alone. This suggests a strong effect of arabinan-rich RG-I pectin on the microbiome. A similar microbiota community modulation pattern was observed in response to CD-CP and CD-DWRP (Fig. 3b). They both have lower RG-I content and branching. Overall, the results suggest that the structure

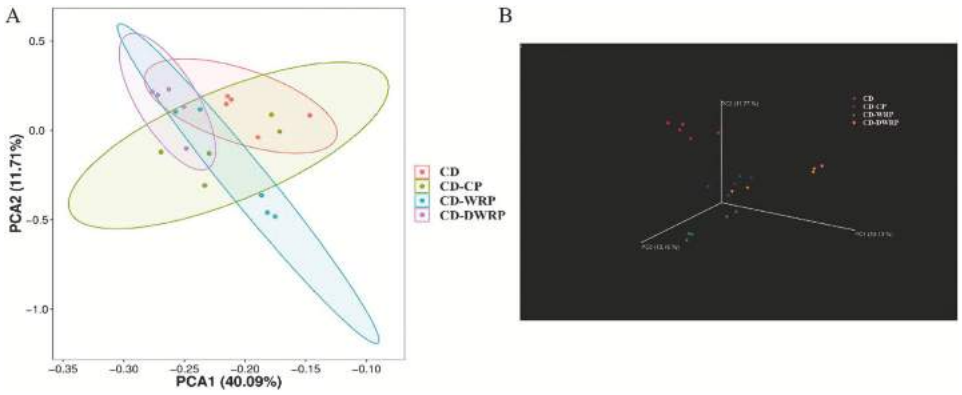

Fig. 3 Response of the caecal and colonic gut microbiota structure to CP, WRP and DWRP treatment. PCA score plot for the caecal content (A), 3D-PCoA of the caecal content (B).

(M_w, branching) and composition (RG-I/HG/arabinose content) of pectin are important factors in the modulation of gut microbiota in C57BL/6J mice.

Bacterial populations of all four diet groups were then compared at the phylum, class and genus levels (Fig. 4). At the phylum level, the dominant bacterial communities were Firmicutes and Bacteroidetes (Fig. 4A). The Bacteroidetes group is a major group responsible for polysaccharide degradation, while the Firmicutes group possesses less polysaccharide-degrading enzymes.[48] In addition, WRP and DWRP were found to have differing effects on the abundance of Actinobacteria (Fig. 4A). WRP significantly decreased the abundance of Actinobacteria, which was increased by DWRP and was even higher than the CD group.

At the class level, the dominant bacteria were classified into Clostridia, Bacteroidia, Deltaproteobacteria and Actinobacteria, with a smaller proportion of Erysipelotrichia, Bacilli and Epsilonproteobacteria (Fig. 4B). At the genus level, the dominant bacteria were classified into *Porphyromonadaceae*, *Desulfovibrio*, *Lachnospiraceae*, *Lachnoclostridium*, *Bacteroides*, *Ruminococcaceae*, *Lactobacillus* and *Oscillospira* (Fig. 4C). To a lesser extent, *Butyrivibrio*, *Ruminococcus*, *Acetatifactor*, *Olsenella* and *Allobaculum* were also found in different proportions in these four groups (Fig. 4C).

3.3 Key phylotypes of gut microbiota modulated by supplementation of chow with WRP and DWRP

To identify the specific bacteria that were modulated in response to different pectin types, the linear discriminant analysis (LDA) effect size (LEFse) analysis was performed. The taxonomic cladogram and LDA score obtained from LEFse analysis identified and visualized the modulatory effect of CP, WRP and DWRP on caecal microbiota (Fig. 5 and 6 and Fig. S4†). At the genus level, a pairwise comparison of the caecal microbiota of the CD-CP, CD-WRP and CD-DWRP groups showed that WRP treatment significantly promoted the growth of *Bacteroides* spp. and its next-generations, such as *Bacteroides caecimuris*, *Bacteroides_ovatus*, and the Ruminococcaceae family, especially its next-generation such as *Ruminococcus* spp., *Butyricicoccus* spp. in the caecal microbiota of C57BL/6J mice. DWRP significantly increased the abundance of *Bifidobacterium* spp., *Lactobacillus* spp., *Faecalibaculum* spp., *Faecalibaculum rodentium*, and *Bacteroides thetaiotaomicron* (Fig. 6).

DWRP treatment increased the amount of *Bifidobacterium* spp. and *Lactobacillus* spp. by about 3 to 8 fold as compared to the other three groups (Table 2). The amount of *Faecalibaculum* spp. in the CD-DWRP group was increased by 17 to 35 fold as compared to the other two pectin-treated groups. Similarly, the amount of *Ruminococcus* spp. in the CD-WRP group was also significantly increased by 5 fold as compared to the CD group. At the family level, WRP treatment significantly promoted the growth of the Ruminococcaceae family, Desulfovibrionaceae family and Bacteroidales family, while the DWRP treatment significantly increased the abundance of the Clostridiales family, Erysipelotrichaceae family and Coriobacteriaceae family (Fig. 5 and 6). More specifically, the amount of Ruminococcaceae family was increased by 16 fold in the CD-WRP group as compared to the CD group (Table 2). At the class level, the CP and DWRP showed significant increases in the abundance of Deltaproteobacteria, Actinobacteria, and Erysipelotrichia, respectively, while the CD-WRP group showed their insignificant decrease in abundance (Fig. 4). However, at the phylum level, only the Actinobacteria were discovered to be increased by DWRP, no significant change in the phylum structure of the caecal microbiota was found after CP or WRP intervention (Fig. 4 and Fig. S4†). WRP and DWRP have a more specific and potentially beneficial effect on the caecal microbiota as compared to CP, though they resulted in discrepant modulations of gut microbiota.

The Ruminococcaceae family is one of the benign autochthonous species that resides in the caecum and the colon.[49] As short chain fatty acid (SCFA) producers, they have been clarified to be responsible for the degradation of various

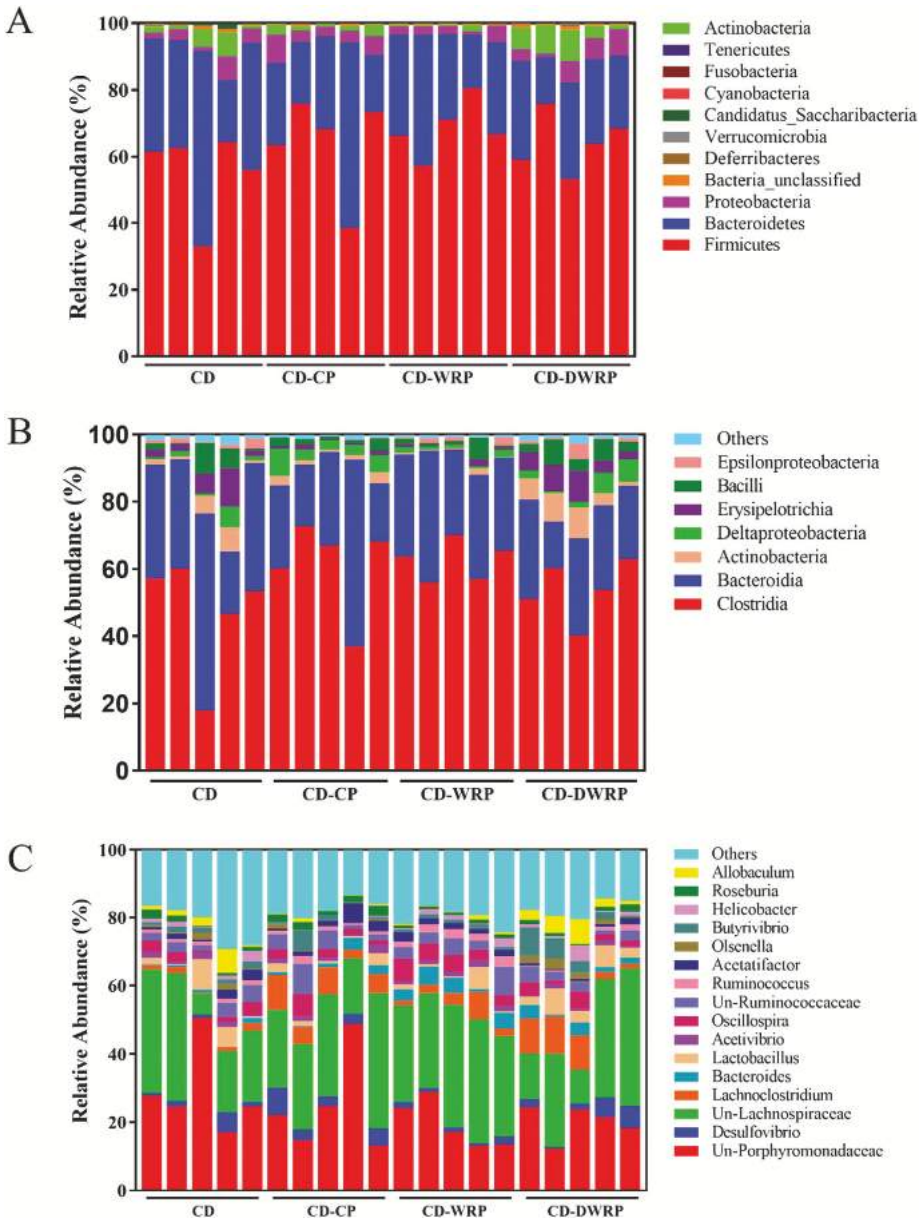

Fig. 4 Structural composition of gut microbiota among all mice groups. (a) Caecal microbiota in CD, CD-CP, CD-WRP and CD-DWRP groups at the phylum level; (b) cecal microbiota in CD, CD-CP, CD-WRP and CD-DWRP groups at the class level; (c) caecal microbiota in CD, CD-CP, CD-WRP and CD-DWRP groups at the genus level.

polysaccharides.[50–53] In the CD-WRP group, the Ruminococcaceae family was significantly increased, and their population size was inversely correlated with increased intestinal permeability,[54] high blood triglycerides[55] and obesity.[53] Among the Ruminococcaceae family, *Ruminococcus* spp. and *Butyricicoccus* spp. were significantly enriched. *Ruminococcus* spp., whose fermentation metabolite is acetate, was also reported to be enriched by the oral administration of established prebiotics like inulin.[56] *Butyricicoccus* spp., with butyrate-producing activity, have been reported to be beneficial bacteria that can suppress inflammation-related diseases.[57] Members of the *Bacteroides* spp. can utilize nearly all of the major plant glycans, including the most complex RG-I and RG-II regions.[58,59] In particular, *Bacteroides thetaiotaomicron* were elucidated to have a large RGI-PUL (polysaccharide utilization location) and galacturan-PUL; thus, they can utilize the RG-I backbone and galacturan side chains.[58] Furthermore, 60% of the *Bacteroides* spp. are capable of degrading arabinan side chains in the RG-I region.[60] Therefore, the average abundance of *Bacteroides* spp. is successively higher in the caecal

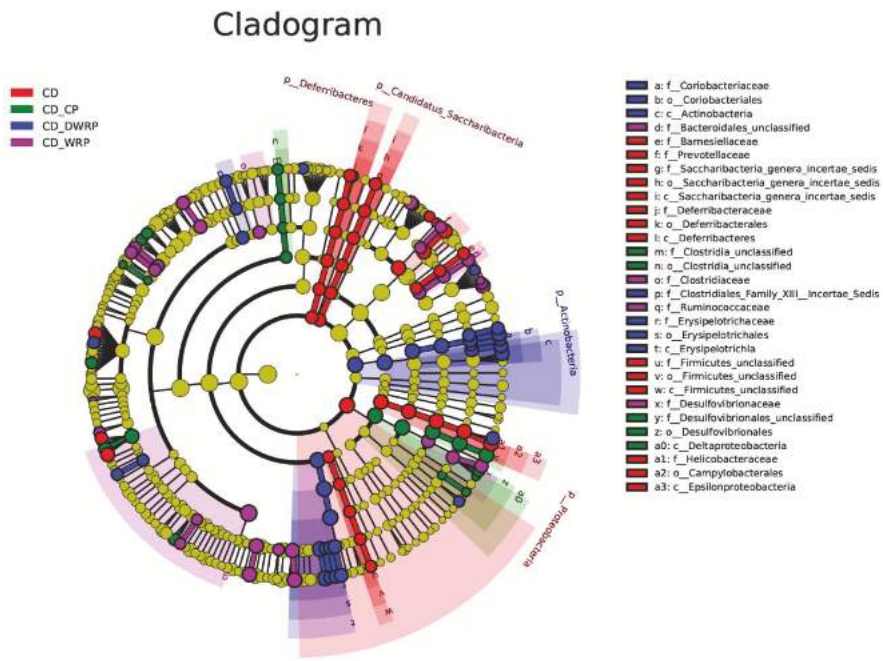

Fig. 5 The taxonomic cladogram obtained from the LEFse analysis of gut microbiota in different groups. Taxonomic cladogram of caecal microbiota in CD, CD-CP, CD-WRP and CD-DWRP groups.

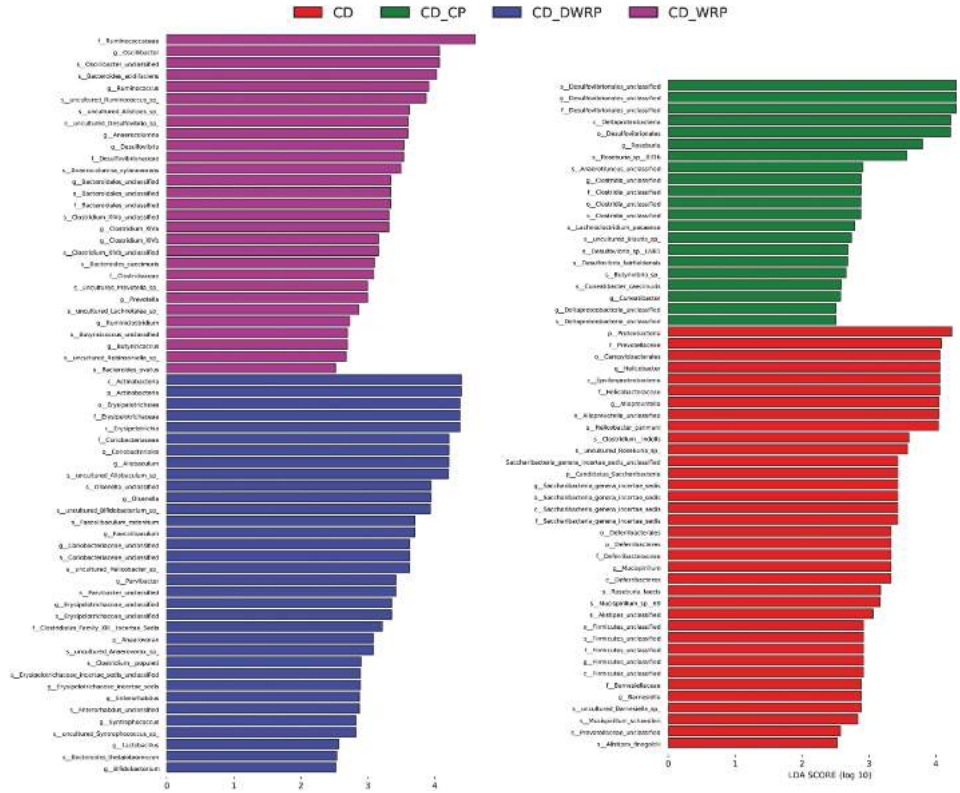

Fig. 6 The LDA score obtained from LEFse analysis of gut microbiota in different groups. The LDA effect size of more than 2.5 was used as a threshold for the LEFse analysis.

Table 2 The abundance of key phylotypes of gut microbiota modulated by dietary CP, WRP and DWRP in CD-fed mice

Key phylotypes	CD	CD-CP	CD-WRP	CD-DWRP
g_*Bifidobacterium*	0.87 ± 1.32^{ab}	0.44 ± 0.33^{a}	0.26 ± 0.37^{a}	2.09 ± 1.83^{b}
g_*Lactobacillus*	1.64 ± 2.27^{a}	1.70 ± 1.15^{a}	2.34 ± 2.03^{a}	4.46 ± 2.03^{b}
g_ *Faecalibaculum*	0.37 ± 0.36^{a}	0.06 ± 0.05^{a}	0.03 ± 0.02^{a}	1.05 ± 0.67^{b}
g_*Bacteroides*	0.55 ± 0.53^{a}	1.62 ± 1.34^{ab}	2.85 ± 2.14^{b}	2.27 ± 1.49^{ab}
g_*Ruminococcus*	1.12 ± 0.22^{a}	1.21 ± 0.69^{a}	2.34 ± 0.57^{b}	0.72 ± 0.64^{a}
f_Ruminococcaceae	1.10 ± 0.61^{a}	12.68 ± 7.17^{bc}	17.58 ± 3.32^{c}	9.97 ± 2.41^{b}
g_*Clostridium_XlVa*	0.12 ± 0.12^{a}	0.31 ± 0.30^{ab}	0.48 ± 0.30^{b}	0.17 ± 0.16^{ab}
g_*Desulfovibrio*	0.24 ± 0.17^{a}	0.14 ± 0.06^{a}	0.78 ± 0.34^{b}	0.21 ± 0.11^{a}

Data representing relative abundance (the percentage of bacteria) of the key phylotypes of gut microbiota are expressed as the mean ± SD ($n = 6$). The means with different superscript represent statistically significant results ($p < 0.05$) based on one-way analysis of variance (ANOVA) with Duncan's range tests, whereas means labeled with the same superscript correspond to results that show no statistically significant differences.

samples from mice supplemented with CP, WRP and DWRP with sequentially higher RG-I and arabinan side chain content (Table 2). *Desulfovibrio* spp. was decreased in obese hosts,[61,62] *Clostridium_XlVa* spp. was enriched in the healthy mice as compared to tumor-bearing mice.[63] Since dietary WRP significantly increased the amount of *Desulfovibrio* spp. and *Clostridium_XlVa* spp., further studies are needed to explore whether the oral administration of WRP could be beneficial for ameliorating obesity or colon cancer.

As the main prebiotics, *Bifidobacterium* and *Lactobacillus* are both crucial for the maintenance of healthy homeostasis.[64] DWRP significantly enriched *Bifidobacterium* and *Lactobacillus*, which is consistent with the previous research where the pectin fraction (with low M_w of 3000–4000 Da) from the parent citrus pectin showed much better prebiotic activity.[32] This could be due to the increased solubility or accessibility of the pectic backbone (due to fewer branches) to microbial degrading enzymes. Besides, *Faecalibaculum rodentium*, as a potentially important species, was also significantly enriched by DWRP (Table 2). It has higher fermentation ability, especially for butyrate production, and is hypothesized to be the main replacer of *Lactobacillus* and *Bifidobacterium* between the early and late stages of life, along with a shift from lactate metabolism to increased SCFA production and carbohydrate metabolism.[65]

The oral administration of DWRP, rather than CP or WRP, enriched the amount of prebiotic microbiota. In another previous study, six pectic oligosaccharides standing for specific substructure within pectin and the parent polysaccharides were evaluated for their fermentation properties.[66] Neutral sugar fractions were discovered to lead to an increase in *Bifidobacterium* populations and higher organic acid yields. Besides, arabinan, galactan, oligoarabinosides and oligogalactosides were the most selective substrates for bifidobacteria. Collectively, pectin with low M_w and higher neutral sugar content better promote the growth of beneficial bacteria.[66,67] Therefore, the prebiotic activity of DWRP is probably due to its high RG-I content and low M_w.

3.4 Effects of citrus pectin with different RG-I content on SCFAs

SCFAs are the end products of the fermentation of dietary fibres by specific anaerobic intestinal microbiota.[68,69] Accumulating evidence suggests that SCFAs play a crucial and favourable role in host physiology and energy homeostasis.[70,71] Acetate, propionate and butyrate are the most abundant components of SCFAs (constitute >95% of the SCFA content), while formate, caproate and valerate are present in substantially lower amounts and make up the remaining <5%.[72]

In the current study, the level of total SCFAs was found to be higher in both the caecum and faeces of CD-WRP and CD-DWRP group compared with the CD group, while that of CD-CP group was higher in the caecum but slightly lower in faeces (Fig. 7). It was in line with reports that some polysaccharides increased SCFA production both *in vivo* and *in vitro*,[73–76] indicating that the gut-derived SCFAs together with gut microbiota modulation may contribute to the beneficial effects of WRP and DWRP.

The CD-CP group contained significantly higher concentrations of acetate (30.32 ± 3.23 μmol g^{-1}) and total SCFAs (41.49 ± 12.24 μmol g^{-1}) as compared to the CD group with acetate concentration of 12.51 ± 2.46 μmol g^{-1} and total SCFA concentration of 26.68 ± 4.52 μmol g^{-1} in the caecum (Fig. 7A, Table S4†), while this trend was surprisingly reversed in the colon (Fig. 7B). The production of acetate and butyrate was reported as being promoted by the fermentation of galacturonic acid and xylose, while the production of propionate was promoted by arabinose and glucose fermentation.[77] Collectively, the increase in acetate and butyrate in the caecum might be due to the fermentation of GalA in CP. Interestingly, the CD-WRP and CD-DWRP group showed no significant increase in concentration for total SCFAs or any kind of SCFAs in the caecal content, while the CD-WRP group significantly increased the concentrations of total SCFAs (28.35 ± 4.65 μmol g^{-1}) and acetate (20.57 ± 2.09 μmol g^{-1}) as compared to the CD group with total SCFA concentration of 20.43 ± 2.09 μmol g^{-1} and acetate concentration of 13.69 ± 1.58 μmol g^{-1} in the colon (Fig. 7B, Table S5†). The slight increase in the production of propionate in CD-WRP and CD-DWRP was mainly due to the fermentation of relatively higher content of Rha and other neutral sugars in RG-I,[13] which was also proven by the strong correlation between *Bacteroides* spp. and the propionate content in the caecum (Fig. S6†). However, the SCFAs in the colonic content seemed not to be successively affected by CP and DWRP, which may be due to the smaller amount of CP and DWRP reaching the colon. Therefore, we tentatively

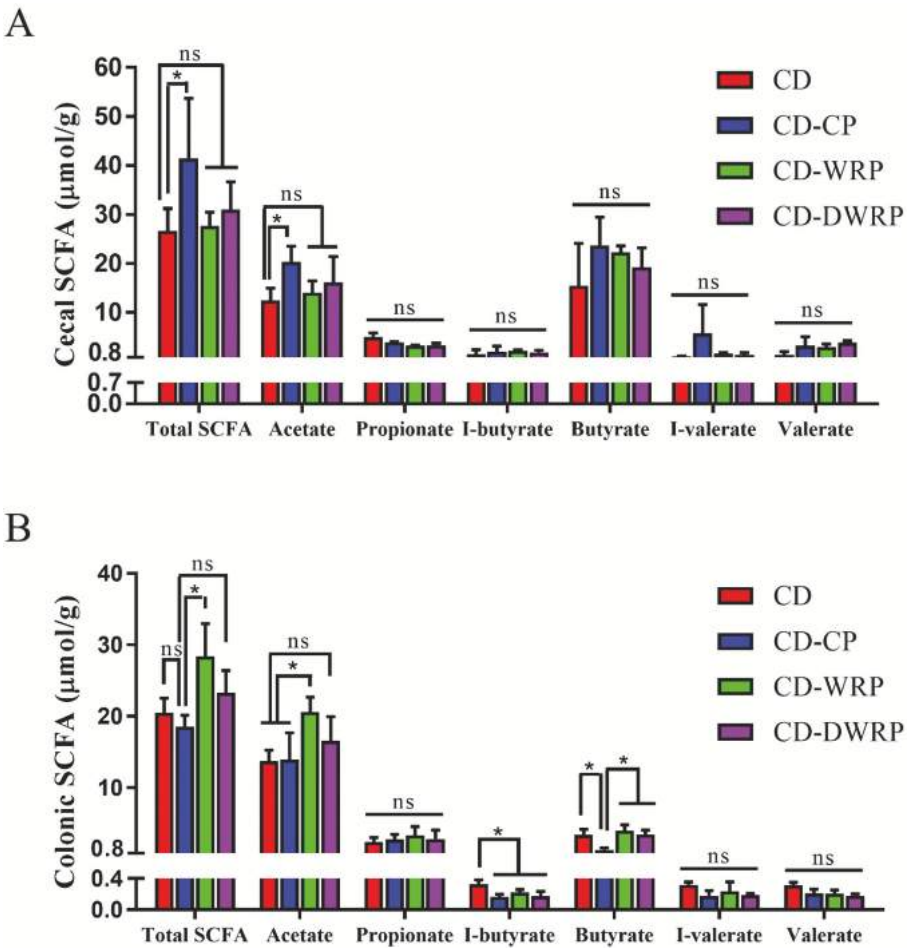

Fig. 7 The concentration (μmol g^{-1}) of acetic, propionate, butyrate, I-butyrate, valerate, and I-valerate in the caecal contents (A) and colon faeces (B) of the pectin treated group and chow diet group. *$P < 0.05$; ns, not significant.

presumed that there was a sequential degradative model of pectin enrichment in different regions of the lower digestive tract, which was consistent with what was previously pointed out for complex glycan and arabinogalactan depolymerisation.[59] It is possible that the RG-I-enriched pectin, with large M_w (WRP as a typical representative), arabinose and galacturonan side chains in the RG-I region, was firstly fermented in the caecum, then the remaining RG-I fraction was transferred to the colon and subsequently fermented. For the HG-enriched pectin with high M_w and limited side chain content (CP as a typical representative), the caecum was the main fermentation location since only a small amount could reach the colon. For pectin with relatively higher RG-I content and lower M_w (DWRP as a typical representative), it could be partly fermented in the caecum, while some could reach the colon.

3.5 Growth performance and biochemical parameters in response to dietary WRP and DWRP supplementation

After a 9-week intervention, three pectin intervention groups all had lower body weight and body weight gain as compared to the CD group (Fig. 8B). Additionally, the weight gain of the CD-WRP group was the lowest. As indicated previously, dietary polysaccharides with a prebiotic effect are capable of decreasing the body weight as well as food intake of experimental mice.[69,78] Here, dietary CP, WRP and DWRP were found to significantly decrease the body weight gain while no significant change in the food intake was discovered for four groups of mice (Fig. S5†). Unlike the fucoidan group, which was reported to lose weight due to the promotion of satiety,[79] both CD-WRP and CD-DWRP groups had similar average food intake to the CD group, and therefore the decrease in weight gain was not due to a reduction in the energy intake. Besides, pectin can delay gastric emptying, slow intestinal transport and affect the mixing of food and digestive enzymes, thus affecting the digestion and absorption of carbohydrates and fats.[80] Given that the characteristic bacteria in lean hosts, such as *Desulfovibrio* spp., *Bifidobacterium* spp. and *Clostridium_XlVa* spp., were largely enriched with WRP and DWRP, and elevated concentrations of SCFAs could regulate energy homeostasis, the weight loss in these two groups could be partly due to WRP

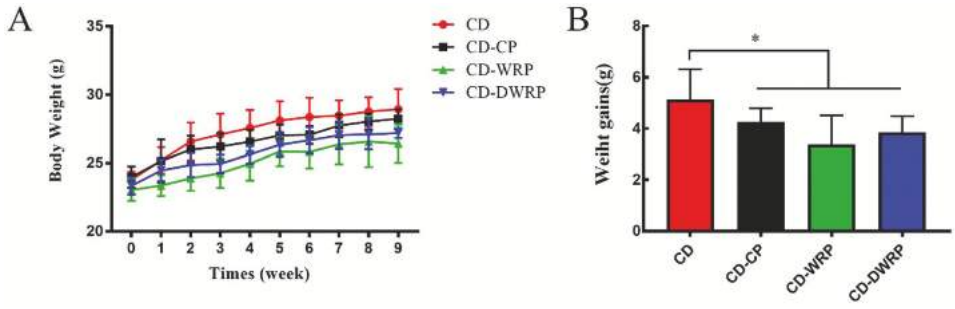

Fig. 8 Growth performance (A) and weight gain (B) of mice in response to dietary CP, WRP and DWRP. *$P < 0.05$.

and DWRP both stimulating beneficial gut microbiota, especially SCFA-producing ones, thus increasing the levels of total SCFAs in the colon.

Considering that there is a strong correlation between SCFAs and the mediation of inflammation and energy metabolism,[69] the levels of lipid and inflammatory cytokines from all mice were analyzed (Table S6†). Significant decreases in inflammatory cytokine levels, including lipopolysaccharides (LPS) and Tumour Necrosis Factor-α (TNF-α), were found in both the CD-WRP and CD-DWRP groups (Table S6†). The discrepancy among the three groups was probably due to the discriminating modulation of gut microbiota resulting from different structural features (Fig. 3B and 4). When LPS is absorbed and enters into the circulatory system, the inflammatory response of the host is triggered;[81] therefore, taken together, the prebiotic activity by RG-I-enriched DWRP in C57BL/6J mice is mainly mediated by the marked structure modulation of the gut microbiota, which includes inhibiting a wide range of intestinal microbes and enriching some SCFA producers, and at least in part, by elevating SCFA levels in the colon as well as reducing serum LPS levels.

4. Conclusion

By enriching the prebiotic bacteria including *Bifidobacterium* spp. and *Lactobacillus* spp., and SCFA producing bacteria, *Faecalibacterium* spp., the dietary DWRP showed the best potential prebiotic effect. Dietary WRP mainly enriched SCFA-producing bacteria, including the Ruminococcaceae family, especially *Ruminococcus* spp., *Butyricicoccus* spp. as well as *Bacteroides* spp., which are mainly responsible for arabinan side chain degradation. WRP and DWRP modulate the gut microbiota beneficial for the host in a structure-dependent path. Collectively, high RG-I content and low M_w will be more beneficial to the intestinal microbial ecology. Besides, the CD-WRP group showed the most pronounced caecal microbiota structural shift as compared to the CD group, demonstrating the strong effect of arabinan-rich RG-I pectin on the modulation of caecal microbiota. Besides, based on the comparison of specific SCFAs in caecum and colon, we tentatively hypothesize that WRP were probably being sequentially utilized in the caecum and colon, while CP was mainly fermented in the caecum. By providing new insights into the well-proven beneficial effects of RG-I-enriched pectin in the positive modulation of gut microbiota, our results rationalize that the RG-I-enriched pectin with low M_w could be commercially used as a novel prebiotic substrate by manipulating the gut microbiota.

Author contributions

G.Z.M. designed experiments, performed the animal studies and statistical analysis and wrote the manuscript, S.G.C. and X.Q.Y. provided the funding and insightful suggestions to the work. S.L. helped to take care of the animals and performed the OGTT. C. O. and R.J.L. improved the language of this manuscript. All authors read and approved the final manuscript.

Conflicts of interest

There are no conflicts of interest to declare.

Acknowledgements

This work was finacially supported in part by National Key Research and Development program of China (2017YFE0122300) and National Natural Science Foundation of China (31871815).

References

1 D. Wu, Y. Cao, J. Chen, H. Gao, X. Ye, D. Liu and S. Chen, Feasibility study on water reclamation from the sorting/grading operation in mandarin orange canning production, *J. Cleaner Prod.*, 2016, **113**, 224–230.
2 J. Chen, H. Cheng, D. Wu, R. J. Linhardt, Z. Zhi, L. Yan, S. Chen and X. Ye, Green recovery of pectic polysaccharides from citrus canning processing water, *J. Cleaner Prod.*, 2017, **144**, 459–469.
3 D. Mohnen, Pectin structure and biosynthesis, *Curr. Opin. Plant Biol.*, 2008, **11**, 266–277.

4 F. Buffetto, V. Cornuault, M. G. Rydahl, D. Ropartz, C. Alvarado, V. Echasserieau, S. Le Gall, B. Bouchet, O. Tranquet, Y. Verhertbruggen, W. G. Willats, J. P. Knox, M. C. Ralet and F. Guillon, The Deconstruction of Pectic Rhamnogalacturonan I Unmasks the Occurrence of a Novel Arabinogalactan Oligosaccharide Epitope, *Plant Cell Physiol.*, 2015, **56**, 2181–2196.

5 A. Noreen, Z. I. Nazli, J. Akram, I. Rasul, A. Mansha, N. Yaqoob, R. Iqbal, S. Tabasum, M. Zuber and K. M. Zia, Pectins functionalized biomaterials; a new viable approach for biomedical applications: A review, *Int. J. Biol. Macromol.*, 2017, **101**, 254–272.

6 E. D. Ngouémazong, S. Christiaens, A. Shpigelman, A. Van Loey and M. Hendrickx, The Emulsifying and Emulsion-Stabilizing Properties of Pectin: A Review, *Compr. Rev. Food Sci. Food Saf.*, 2015, **14**, 705–718.

7 T. Zhang, Y. Lan, Y. Zheng, F. Liu, D. Zhao, K. H. Mayo, Y. Zhou and G. Tai, Identification of the bioactive components from pH-modified citrus pectin and their inhibitory effects on galectin-3 function, *Food Hydrocolloids*, 2016, **58**, 113–119.

8 H. Zhang, J. Chen, J. Li, L. Yan, S. Li, X. Ye, D. Liu, T. Ding, R. J. Linhardt, C. Orfila and S. Chen, Extraction and characterization of RG-I enriched pectic polysaccharides from mandarin citrus peel, *Food Hydrocolloids*, 2018, **79**, 579–586.

9 Z. Zhi, J. Chen, S. Li, W. Wang, R. Huang, D. Liu, T. Ding, R. J. Linhardt, S. Chen and X. Ye, Fast preparation of RG-I enriched ultra-low molecular weight pectin by an ultrasound accelerated Fenton process, *Sci. Rep.*, 2017, **7**, 541.

10 M. Meijerink, C. Rosch, N. Taverne, K. Venema, H. Gruppen, H. A. Schols and J. M. Wells, Structure Dependent-Immunomodulation by Sugar Beet Arabinans via a SYK Tyrosine Kinase-Dependent Signaling Pathway, *Front. Immunol.*, 2018, **9**, 1972.

11 N. Khodaei, B. Fernandez, I. Fliss and S. Karboune, Digestibility and prebiotic properties of potato rhamnogalacturonan I polysaccharide and its galactose-rich oligosaccharides/oligomers, *Carbohydr. Polym.*, 2016, **136**, 1074–1084.

12 A. Ferreira-Lazarte, F. J. Moreno, C. Cueva, I. Gil-Sanchez and M. Villamiel, Behaviour of citrus pectin during its gastrointestinal digestion and fermentation in a dynamic simulator (simgi(R)), *Carbohydr. Polym.*, 2019, **207**, 382–390.

13 N. Larsen, C. B. Souza, L. Krych, T. B. Cahu, M. Wiese, W. Kot, K. M. Hansen, A. Blennow, K. Venema and L. Jespersen, Potential of Pectins to Beneficially Modulate the Gut Microbiota Depends on Their Structural Properties, *Front. Microbiol.*, 2019, **10**, 223.

14 F. Sommer and F. Backhed, The gut microbiota–masters of host development and physiology, *Nat. Rev. Microbiol.*, 2013, **11**, 227–238.

15 A. Heintz-Buschart and P. Wilmes, Human Gut Microbiome: Function Matters, *Trends Microbiol.*, 2018, **26**, 563–574.

16 K. Matsuoka and T. Kanai, The gut microbiota and inflammatory bowel disease, *Semin. Immunopathol.*, 2015, **37**, 47–55.

17 J. Halfvarson, C. J. Brislawn, R. Lamendella, Y. Vazquez-Baeza, W. A. Walters, L. M. Bramer, M. D'Amato, F. Bonfiglio, D. McDonald, A. Gonzalez, E. E. McClure, M. F. Dunklebarger, R. Knight and J. K. Jansson, Dynamics of the human gut microbiome in inflammatory bowel disease, *Nat. Microbiol.*, 2017, **2**, 17004.

18 A. S. Meijnikman, V. E. Gerdes, M. Nieuwdorp and H. Herrema, Evaluating Causality of Gut Microbiota in Obesity and Diabetes in Humans, *Endocr. Rev.*, 2018, **39**, 133–153.

19 K. H. Allin, V. Tremaroli, R. Caesar, B. A. H. Jensen, M. T. F. Damgaard, M. I. Bahl, T. R. Licht, T. H. Hansen, T. Nielsen, T. M. Dantoft, A. Linneberg, T. Jorgensen, H. Vestergaard, K. Kristiansen, P. W. Franks, I. D. consortium, T. Hansen, F. Backhed and O. Pedersen, Aberrant intestinal microbiota in individuals with prediabetes, *Diabetologia*, 2018, **61**, 810–820.

20 H. Chu, Y. Duan, L. Yang and B. Schnabl, Small metabolites, possible big changes: a microbiota-centered view of non-alcoholic fatty liver disease, *Gut*, 2019, **68**, 359–370.

21 F. Z. Marques, C. R. Mackay and D. M. Kaye, Beyond gut feelings: how the gut microbiota regulates blood pressure, *Nat. Rev. Cardiol.*, 2018, **15**, 20–32.

22 C. L. Boulange, A. L. Neves, J. Chilloux, J. K. Nicholson and M. E. Dumas, Impact of the gut microbiota on inflammation, obesity, and metabolic disease, *Genome Med.*, 2016, **8**, 42.

23 L. J. Kasselman, N. A. Vernice, J. DeLeon and A. B. Reiss, The gut microbiome and elevated cardiovascular risk in obesity and autoimmunity, *Atherosclerosis*, 2018, **271**, 203–213.

24 Z. Jie, H. Xia, S. L. Zhong, Q. Feng, S. Li, S. Liang, H. Zhong, Z. Liu, Y. Gao, H. Zhao, D. Zhang, Z. Su, Z. Fang, Z. Lan, J. Li, L. Xiao, J. Li, R. Li, X. Li, F. Li, H. Ren, Y. Huang, Y. Peng, G. Li, B. Wen, B. Dong, J. Y. Chen, Q. S. Geng, Z. W. Zhang, H. Yang, J. Wang, J. Wang, X. Zhang, L. Madsen, S. Brix, G. Ning, X. Xu, X. Liu, Y. Hou, H. Jia, K. He and K. Kristiansen, The gut microbiome in atherosclerotic cardiovascular disease, *Nat. Commun.*, 2017, **8**, 845.

25 Z. H. Shen, C. X. Zhu, Y. S. Quan, Z. Y. Yang, S. Wu, W. W. Luo, B. Tan and X. Y. Wang, Relationship between intestinal microbiota and ulcerative colitis: Mechanisms and clinical application of probiotics and fecal microbiota transplantation, *World J. Gastroenterol.*, 2018, **24**, 5–14.

26 D. W. Kang, J. B. Adams, A. C. Gregory, T. Borody, L. Chittick, A. Fasano, A. Khoruts, E. Geis, J. Maldonado, S. McDonough-Means, E. L. Pollard, S. Roux, M. J. Sadowsky, K. S. Lipson, M. B. Sullivan, J. G. Caporaso and R. Krajmalnik-Brown, Microbiota Transfer Therapy alters gut ecosystem and improves gastrointestinal and autism symptoms: an open-label study, *Microbiome*, 2017, **5**, 10.

27 C. J. Chang, C. S. Lin, C. C. Lu, J. Martel, Y. F. Ko, D. M. Ojcius, S. F. Tseng, T. R. Wu, Y. Y. Chen, J. D. Young and H. C. Lai, Ganoderma lucidum reduces obesity in mice by modulating the composition of the gut microbiota, *Nat. Commun.*, 2015, **6**, 7489.

28 N. Khodaei and S. Karboune, Enzymatic generation of galactose-rich oligosaccharides/oligomers from potato rhamnogalacturonan I pectic polysaccharides, *Food Chem.*, 2016, **197**, 406–414.

29 A. J. Svagan, A. Kusic, C. De Gobba, F. H. Larsen, P. Sassene, Q. Zhou, M. van de Weert, A. Mullertz, B. Jorgensen and P. Ulvskov, Rhamnogalacturonan-I Based Microcapsules for Targeted Drug Release, *PLoS One*, 2016, **11**, e0168050.

30 R. Di, M. S. Vakkalanka, C. Onumpai, H. K. Chau, A. White, R. A. Rastall, K. Yam and A. T. Hotchkiss, Jr., Pectic oligosaccharide structure-function relationships: Prebiotics, inhibitors of Escherichia coli O157:H7 adhesion and reduction of Shiga toxin cytotoxicity in HT29 cells, *Food Chem.*, 2017, **227**, 245–254.

31 B. Gómez, B. Gullón, R. Yáñez, H. Schols and J. L. Alonso, Prebiotic potential of pectins and pectic oligosaccharides derived from lemon peel wastes and sugar beet pulp: A comparative evaluation, *J. Funct. Foods*, 2016, **20**, 108–121.

32 S. Zhang, H. Hu, L. Wang, F. Liu and S. Pan, Preparation and prebiotic potential of pectin oligosaccharides obtained from citrus peel pectin, *Food Chem.*, 2018, **244**, 232–237.

33 J. Li, S. Li, Y. Zheng, H. Zhang, J. Chen, L. Yan, T. Ding, R. J. Linhardt, C. Orfila, D. Liu, X. Ye and S. Chen, Fast preparation of rhamnogalacturonan I enriched low molecular weight pectic polysaccharide by ultrasonically accelerated metal-free Fenton reaction, *Food Hydrocolloids*, 2019, **95**, 551–561.

34 D. J. Strydom, Chromatographic separation of 1-phenyl-3-methyl-5-pyrazolone-derivatized neutral, acidic and basic aldoses, *J. Chromatogr. A*, 1994, **678**, 17–23.

35 D. W. Fadrosh, B. Ma, P. Gajer, N. Sengamalay, S. Ott, R. M. Brotman and J. Ravel, An improved dual-indexing approach for multiplexed 16S rRNA gene sequencing on the Illumina MiSeq platform, *Microbiome*, 2014, **2**, 6.

36 T. R. Wu, C. S. Lin, C. J. Chang, T. L. Lin, J. Martel, Y. F. Ko, D. M. Ojcius, C. C. Lu, J. D. Young and H. C. Lai, Gut commensal Parabacteroides goldsteinii plays a predominant role in the anti-obesity effects of polysaccharides isolated from Hirsutella sinensis, *Gut*, 2019, **68**, 248–262.

37 L. Zhang, X. Ye, T. Ding, X. Sun, Y. Xu and D. Liu, Ultrasound effects on the degradation kinetics, structure and rheological properties of apple pectin, *Ultrason. Sonochem.*, 2013, **20**, 222–231.

38 W. Burchard, Solution Properties of Branched Macromolecules, *Adv. Polym. Sci.*, 1999, **143**, 113–194.

39 S. Podzimek, T. Vlcek and C. Johann, Characterization of branched polymers by size exclusion chromatography coupled with multiangle light scattering detector. I. Size exclusion chromatography elution behavior of branched polymers, *J. Appl. Polym. Sci.*, 2001, **81**, 1588–1594.

40 G. Robinson, S. B. Ross-Murphy and E. R. Morris, Viscosity-molecular weight relationships, intrinsic chain flexibility, and dynamic solution properties of guar galactomannan, *Carbohydr. Res.*, 1982, **107**, 17–32.

41 J. Wang and L. Zhang, Structure and chain conformation of five water-soluble derivatives of a beta-D-glucan isolated from Ganoderma lucidum, *Carbohydr. Res.*, 2009, **344**, 105–112.

42 A. N. Round, A. J. MacDougall, S. G. Ring and V. J. Morris, Unexpected branching in pectin observed by atomic force microscopy, *Carbohydr. Res.*, 1997, **303**, 251–253.

43 M. Jin, S. Kalainy, N. Baskota, D. Chiang, E. C. Deehan, C. McDougall, P. Tandon, I. Martinez, C. Cervera, J. Walter and J. G. Abraldes, Faecal microbiota from patients with cirrhosis has a low capacity to ferment non-digestible carbohydrates into short-chain fatty acids, *Liver Int.*, 2019, 1437–1447.

44 X. Xu and X. Zhang, Lentinula edodes-derived polysaccharide alters the spatial structure of gut microbiota in mice, *PLoS One*, 2015, **10**, e0115037.

45 P. Kungel, V. G. Correa, R. C. G. Correa, R. A. Peralta, M. Sokovic, R. C. Calhelha, A. Bracht, I. Ferreira and R. M. Peralta, Antioxidant and antimicrobial activities of a purified polysaccharide from yerba mate (Ilex paraguariensis), *Int. J. Biol. Macromol.*, 2018, **114**, 1161–1167.

46 E. Dahdouh, S. El-Khatib, E. Baydoun and R. M. Abdel-Massih, Additive Effect of MCP in Combination with Cefotaxime Against Staphylococcus aureus, *Med. Chem.*, 2017, **13**, 682–688.

47 T. Stalheim, S. Ballance, B. E. Christensen and P. E. Granum, Sphagnan–a pectin-like polymer isolated from Sphagnum moss can inhibit the growth of some typical food spoilage and food poisoning bacteria by lowering the pH, *J. Appl. Microbiol.*, 2009, **106**, 967–976.

48 M. A. Mahowald, F. E. Rey, H. Seedorf, P. J. Turnbaugh, R. S. Fulton, A. Wollam, N. Shah and B. L. Cantarel, Characterizing a model human gut microbiota composed of members of its two dominant bacterial phyla, *Proc. Natl. Acad. Sci.*, 2009, **106**, 5859–5864.

49 G. P. Donaldson, S. M. Lee and S. K. Mazmanian, Gut biogeography of the bacterial microbiota, *Nat. Rev. Microbiol.*, 2016, **14**, 20–32.

50 H. Zeng, C. Huang, S. Lin, M. Zheng, C. Chen, B. Zheng and Y. Zhang, Lotus Seed Resistant Starch Regulates Gut Microbiota and Increases Short-Chain Fatty Acids Production and Mineral Absorption in Mice, *J. Agric. Food Chem.*, 2017, **65**, 9217–9225.

51 Y. Wang, N. Zhang, J. Kan, X. Zhang, X. Wu, R. Sun, S. Tang, J. Liu, C. Qian and C. Jin, Structural characterization of water-soluble polysaccharide from Arctium lappa and its effects on colitis mice, *Carbohydr. Polym.*, 2019, **213**, 89–99.

52 S. Hooda, B. M. Boler, M. C. Serao, J. M. Brulc, M. A. Staeger, T. W. Boileau, S. E. Dowd, G. C. Fahey, Jr. and K. S. Swanson, 454 pyrosequencing reveals a shift in fecal microbiota of healthy adult men consuming polydextrose or soluble corn fiber, *J. Nutr.*, 2012, **142**, 1259–1265.

53 A. Salonen, L. Lahti, J. Salojarvi, G. Holtrop, K. Korpela, S. H. Duncan, P. Date, F. Farquharson, A. M. Johnstone, G. E. Lobley, P. Louis, H. J. Flint and W. M. de Vos, Impact of diet and individual variation on intestinal microbiota composition and fermentation products in obese men, *ISME J.*, 2014, **8**, 2218–2230.

54 S. Leclercq, S. Matamoros, P. D. Cani, A. M. Neyrinck, F. Jamar, P. Starkel, K. Windey, V. Tremaroli, F. Backhed, K. Verbeke, P. de Timary and N. M. Delzenne, Intestinal permeability, gut-bacterial dysbiosis, and behavioral markers of alcohol-dependence severity, *Proc. Natl. Acad. Sci. U. S. A.*, 2014, **111**, E4485–E4493.

55 L. M. Cox, I. Cho, S. A. Young, W. H. Anderson, B. J. Waters, S. C. Hung, Z. Gao, D. Mahana, M. Bihan, A. V. Alekseyenko, B. A. Methe and M. J. Blaser, The nonfermentable dietary fiber hydroxypropyl methylcellulose modulates intestinal microbiota, *FASEB J.*, 2013, **27**, 692–702.

56 S. Macfarlane, G. T. Macfarlane and J. H. Cummings, Review article: prebiotics in the gastrointestinal tract, *Aliment. Pharmacol. Ther.*, 2006, **24**, 701–714.

57 S. Devriese, V. Eeckhaut, A. Geirnaert, L. Van den Bossche, P. Hindryckx, T. Van de Wiele, F. Van Immerseel, R. Ducatelle, M. De Vos and D. Laukens, Reduced Mucosa-associated Butyricicoccus Activity in Patients with Ulcerative Colitis Correlates with Aberrant Claudin-1 Expression, *J. Crohns Colitis*, 2017, **11**, 229–236.

58 E. C. Martens, E. C. Lowe, H. Chiang, N. A. Pudlo, M. Wu, N. P. McNulty, D. W. Abbott, B. Henrissat, H. J. Gilbert, D. N. Bolam and J. I. Gordon, Recognition and degradation of plant cell wall polysaccharides by two human gut symbionts, *PLos Biol.*, 2011, **9**, e1001221.

59 D. Ndeh and H. J. Gilbert, Biochemistry of complex glycan depolymerisation by the human gut microbiota, *FEMS Microbiol. Rev.*, 2018, **42**, 146–164.

60 A. S. Luis, J. Briggs, X. Zhang, B. Farnell, D. Ndeh, A. Labourel, A. Basle, A. Cartmell, N. Terrapon, K. Stott, E. C. Lowe, R. McLean, K. Shearer, J. Schuckel, I. Venditto, M. C. Ralet, B. Henrissat, E. C. Martens, S. C. Mosimann, D. W. Abbott and H. J. Gilbert, Dietary pectic glycans are degraded by coordinated enzyme pathways in human colonic Bacteroides, *Nat. Microbiol.*, 2018, **3**, 210–219.

61 C. L. Karlsson, J. Onnerfalt, J. Xu, G. Molin, S. Ahrne and K. Thorngren-Jerneck, The microbiota of the gut in preschool children with normal and excessive body weight, *Obesity*, 2012, **20**, 2257–2261.

62 X. Jiao, Y. Wang, Y. Lin, Y. Lang, E. Li, X. Zhang, Q. Zhang, Y. Feng, X. Meng and B. Li, Blueberry polyphenols extract as a potential prebiotic with anti-obesity effects on C57BL/6 J mice by modulating the gut microbiota, *J. Nutr. Biochem.*, 2019, **64**, 88–100.

63 Y. Luan, D. Mao, M. Chen, *et al.*, Structural changes of gut microbiota in mice with chronic constipation and intestinal tumor, *Biomed. Res.*, 2017, **28**, 10062–10067.

64 T. Cerdo, J. A. Garcia-Santos, G. B. Mercedes and C. Campoy, The Role of Probiotics and Prebiotics in the Prevention and Treatment of Obesity, *Nutrients*, 2019, **11**, 635.

65 S. Lim, D. H. Chang, S. Ahn and B. C. Kim, Whole genome sequencing of "Faecalibaculum rodentium" ALO17, isolated from C57BL/6J laboratory mouse feces, *Gut Pathog.*, 2016, **8**, 3.

66 C. Onumpai, S. Kolida, E. Bonnin and R. A. Rastall, Microbial utilization and selectivity of pectin fractions with various structures, *Appl. Environ. Microbiol.*, 2011, **77**, 5747–5754.

67 J. Chen, R. H. Liang, W. Liu, T. Li, C. M. Liu, S. S. Wu and Z. J. Wang, Pectic-oligosaccharides prepared by dynamic high-pressure microfluidization and their in vitro fermentation properties, *Carbohydr. Polym.*, 2013, **91**, 175–182.

68 T. Aljutaily, M. Consuegra-Fernandez, F. Aranda, F. Lozano and E. Huarte, Gut microbiota metabolites for sweetening type I diabetes, *Cell. Mol. Immunol.*, 2018, **15**, 92–95.

69 Q. Shang, Y. Wang, L. Pan, Q. Niu, C. Li, H. Jiang, C. Cai, J. Hao, G. Li and G. Yu, Dietary Polysaccharide from Enteromorpha Clathrata Modulates Gut Microbiota and Promotes the Growth of Akkermansia muciniphila, Bifidobacterium spp. and Lactobacillus spp, *Mar. Drugs*, 2018, **16**, 167.

70 A. Koh, F. De Vadder, P. Kovatcheva-Datchary and F. Backhed, From Dietary Fiber to Host Physiology: Short-Chain Fatty Acids as Key Bacterial Metabolites, *Cell*, 2016, **165**, 1332–1345.

71 D. Rios-Covian, P. Ruas-Madiedo, A. Margolles, M. Gueimonde, C. G. de Los Reyes-Gavilan and N. Salazar, Intestinal Short Chain Fatty Acids and their Link with Diet and Human Health, *Front. Microbiol.*, 2016, **7**, 185.

72 J. H. Cummings, E. W. Pomare, W. J. Branch, C. P. Naylor and G. T. Macfarlane, Short chain fatty acids in human large intestine, portal, hepatic and venous blood, *Gut*, 1987, **28**, 1221–1227.

73 Q. Nie, J. Hu, H. Gao, L. Fan, H. Chen and S. Nie, Polysaccharide from Plantago asiatica L. attenuates hyperglycemia, hyperlipidemia and affects colon microbiota in type 2 diabetic rats, *Food Hydrocolloids*, 2019, **86**, 34–42.

74 S. Y. Xu, J. J. Aweya, N. Li, R. Y. Deng, W. Y. Chen, J. Tang and K. L. Cheong, Microbial catabolism of Porphyra haitanensis polysaccharides by human gut microbiota, *Food Chem.*, 2019, **289**, 177–186.

75 J. Gao, L. Lin, Z. Chen, Y. Cai, C. Xiao, F. Zhou, B. Sun and M. Zhao, In vitro digestion and fermentation of three polysaccharide fractions from Laminaria japonica and their impact on lipid metabolism-associated human gut microbiota, *J. Agric. Food Chem.*, 2019, **67**(26), 7496–7505.

76 J. L. Hu, S. P. Nie, F. F. Min and M. Y. Xie, Polysaccharide from seeds of Plantago asiatica L. increases short-chain fatty acid production and fecal moisture along with lowering pH in mouse colon, *J. Agric. Food Chem.*, 2012, **60**, 11525–11532.

77 P. B. Mortensen, K. Holtug and H. S. Rasmussen, Short-chain fatty acid production from mono- and disaccharides in a fecal incubation system: implications for colonic fermentation of dietary fiber in humans, *J. Nutr.*, 1988, **118**, 321–325.

78 Q. Shang, X. Shan, C. Cai, J. Hao, G. Li and G. Yu, Dietary fucoidan modulates the gut microbiota in mice by increasing the abundance of Lactobacillus and Ruminococcaceae, *Food Funct.*, 2016, **7**, 3224–3232.

79 E. E. Canfora, J. W. Jocken and E. E. Blaak, Short-chain fatty acids in control of body weight and insulin sensitivity, *Nat. Rev. Endocrinol.*, 2015, **11**, 577–591.

80 C. Di Lorenzo, C. M. Williams, F. Hajnal and J. E. Valenzuela, Pectin delays gastric emptying and increases satiety in obese subjects, *Gastroenterology*, 1988, **95**, 1211–1215.

81 C. Zhang, S. Li, L. Yang, P. Huang, W. Li, S. Wang, G. Zhao, M. Zhang, X. Pang, Z. Yan, Y. Liu and L. Zhao, Structural modulation of gut microbiota in life-long calorie-restricted mice, *Nat. Commun.*, 2013, **4**, 2163.